



# Goat milk concentrated by nanofiltration: flow decline modeling and characterization

Maria Helena Machado CANELLA<sup>1</sup>, Giordana Demaman AREND<sup>1</sup>, Lenilton Santos SOARES<sup>1</sup>,  
Leandro Antunes de Sá PLOÊNCIO<sup>2</sup>, Luciano MOLOGNONI<sup>2</sup>, Heitor DAGUER<sup>2</sup>, Erick Almeida ESMERINO<sup>3</sup>,  
Ramon SILVA<sup>4</sup>, Eduard HERNANDEZ<sup>5</sup>, Elane Schwinden PRUDENCIO<sup>1,6\*</sup> 

## Abstract

The skimmed goat milk was submitted to the nanofiltration process using a volume reduction factor (VRF) equal to 2. It was verified a rapid decrease of the permeate flux at a low time, with a continuous flux, caused by the reversible resistance, which is characterized by the standard and complete blocking. The combined fouling model was evaluated, including complete pore blocking and cake filtration mechanism, which described the skimmed goat milk nanofiltration behavior. For the VRF equal to 2 was determined the total solids, protein, lactose, ash, mineral fraction content, which increased successfully with the nanofiltration process. The Power Law and Herschel-Buckley models were fitting to describe the flow behavior for retentate, which presented the higher apparent viscosity.

**Keywords:** goat milk; membrane separation; concentration; permeate flux; milk components.

**Practical Application:** The skimmed goat milk concentrate obtained from the nanofiltration process retains most of the main milk constituents. This technology has the potential to be used as a pre-concentration step, aiming at obtaining a product with preserved sensory and nutritional qualities with lower production costs. In addition, the clarification of the fouling mechanism involved during the nanofiltration process can be used by the industry to facilitate the milk concentration process.

## 1 Introduction

Goat milk has become popular with consumers because of its low lactose content, high protein content, high calcium content, and a high proportion of more digestible fatty acids compared with cow milk (Chen et al., 2019; Haenlein, 2004). Therefore, is widely used in dairy products because it is highly digestible, is hypoallergenic, and has high nutritional value (Chen et al., 2019), and often even for its taste (Carvalho et al., 2023; Sobral et al., 2023). Santos et al. (2022) highlighted that goat's milk production depends on the animal's fitness, the nutritional value of the food, the level of dry matter intake by the animal, among others. Many types of research were involved in studying the concentration of goat milk, which according to Hariadi et al. (2023a) is used food diversification. Ribeiro et al. (2023) stated that dairy products has been evaluated as an alternative to innovate and improve some quality aspects of the products. According to Hariadi et al. (2023b) milk is a food ingredient that is composed of various nutritional values with balanced proportions. The concentration of milk represents an intermediate processing step in the production of milk products or concentrated milk products, which can be used in several food formulations, such as yogurts, ice cream, bakery products, or some meals, by replacing the use of milk powder, since this material is expensive and requires intensive energy for drying.

Among the concentration processes, highlight the membrane process, which has been successfully investigated for the concentration of milk components. Therefore, the membrane process could be a promising technology for the recovery of fragile compounds in comparison with other concentration processes, which employ higher temperatures. Ng et al. (2017) emphasized that the membrane processes have been demonstrated to be advantageous over the conventional process for the recovery of thermosensitive compounds from milk and cheese whey using the methodologies such as nanofiltration, retaining protein, lactose, and minerals. Moreover, emerging technologies, such as the nanofiltration process, is still innovative for goat milk. However, the nanofiltration of skim milk is particularly susceptible to poor operational efficiency due to flux decline resulting from concentration polarization and fouling. The membrane fouling is due to several possible causes, such as adsorption and blocking of solute on the membrane, formation of a deposited layer on the membrane surface, and composition. Ferrer et al. (2014) cited that during the process, concentration polarization at the membrane surface can rise to a point where the concentrated solutes form a gel layer on the membrane, and this irreversibly decreases the permeation flux and process performance, ultimately causing fouling of the membrane, which is associated with a decline in

Received 10 Dec., 2022

Accepted 25 Jan., 2023

<sup>1</sup> Postgraduate Program in Food Engineering, Technology Center, Universidade Federal de Santa Catarina – UFSC, Florianópolis, SC, Brasil

<sup>2</sup> Advanced Laboratories Section, National Agricultural and Livestock Laboratory, Ministério da Agricultura, Pecuária e Abastecimento, São José, SC, Brasil

<sup>3</sup> Food Technology Department, Universidade Federal Rural do Rio de Janeiro – UFRRJ, Seropédica, RJ, Brasil

<sup>4</sup> Food Department, Instituto Federal do Rio de Janeiro, Rio de Janeiro, RJ, Brasil

<sup>5</sup> Department of Agri-Food Engineering and Biotechnology, Universitat Politècnica de Catalunya BarcelonaTech, Barcelona, Spain

<sup>6</sup> Department of Food Science and Technology, Agricultural Sciences Center, Universidade Federal de Santa Catarina – UFSC, Florianópolis, SC, Brasil

\*Corresponding author: [elane.prudencio@ufsc.br](mailto:elane.prudencio@ufsc.br)

the permeate flux with operation time. As the concentration increases, the permeate fluxes decline (Ferrer et al., 2014).

In this sense, modeling is warranted to quantify the flux decline during concentration that allows the prediction of process behavior (Balyan & Sarkar, 2018). The flow decline modeling and characterization of goat milk by nanofiltration process study is of fundamental importance in the innovation process, as it helps in the efficient technological processes, optimizing time in the development of new products, and according to Silva et al. (2023) with greater assertiveness in the execution and the use of this process by the dairy industry.

Membrane fouling in the dairy industry has generally been attributed to adsorption of proteins and precipitation of calcium phosphate (Ng et al., 2018), but the exact nature of fouling is difficult to ascertain, as this would require some form of in situ and in real-time observation and measurement. Some of the best models known are described by Hermia and Ho and Zydney, which can quite clarify the main reasons for flux decline. Hou et al. (2017) cited that Ho and Zydney developed a combined fouling model considering both pore blocking and the filtration layer to describe flux decline. However, the performance of the nanofiltration process should not only be evaluated regarding the permeate flux and the flux decline but also about the physical, chemical, and rheological properties of the fractions obtained. Thereby, the present study aimed to characterize the performance of the nanofiltration process of skimmed goat milk by evaluating permeate flux decline, fouling resistance, and retentate composition and rheological properties.

## 2 Material and methods

### 2.1 Material

Commercial skim UHT goat milk (Caprilat®, CCA Laticínios, Rio de Janeiro, Brazil) was used as the start material. The skim goat milk composition was  $8.46 \pm 0.01$  g total solids  $100 \text{ g}^{-1}$ ,  $2.91 \pm 0.05$  g total protein  $100 \text{ g}^{-1}$ ,  $3.93 \pm 0.05$  g lactose  $100 \text{ g}^{-1}$  and  $0.89 \pm 0.03$  g ash  $100 \text{ g}^{-1}$ . The initial pH value and titratable acidity were  $6.60 \pm 0.01$  and  $0.12 \pm 0.01$  g  $100 \text{ g}^{-1}$  lactic acid, respectively. All reagents were of analytical grade.

### 2.2 Nanofiltration procedure

The skimmed goat milk was submitted to the nanofiltration process in a pilot filtration unit, using a tangential filtration system and a polyvinylidene fluoride (PVDF) spiral nanofiltration membrane (Osmonics, Minnetonka, MN), with an approximate molar mass cut-off ranging between 150-300 Da, and a filtration area of  $1.2 \text{ m}^2$ . The operating parameters controlled during the nanofiltration process were a temperature of  $25 \pm 1 \text{ }^\circ\text{C}$  and pressure of 700 kPa, up to the volume reduction factor (VRF) of 2 as the endpoint of the process. The VRF was calculated as the ratio between the initial volume (L) of skimmed goat milk used in the feed and the final volume (L) of the concentrate after the nanofiltration process. The permeate flux (J) ( $\text{L}\cdot\text{h}^{-1}\cdot\text{m}^{-2}$ ) was measured at 5 min and removed to obtain the skimmed goat milk concentrate, according to Equation 1:

$$J = \frac{V_p}{t \times A_p} \quad (1)$$

where  $V_p$  (L) is the amount of permeate collected during the period  $t$  (h) and  $A_p$  ( $\text{m}^2$ ) is the permeation surface area of the membrane.

To assess the fouling mechanism during the nanofiltration process, the model of flow decline during filtration can be selected (Hermia, 1982) (Equation 2).

$$d^2 / dV^2 = \beta \left( \frac{dt}{dV} \right)^n \quad (2)$$

where  $V$  is the cumulative volume of filtrate,  $t$  the time of operation, and  $n$  is a constant.

Field et al. (1995) modified the classical constant pressure dead-end filtration equation (Hermia, 1982), which expressed as follows Equation 3:

$$-dJ / dt (J^{n-2}) = K (J - J^*) \quad (3)$$

where  $J^*$  is the steady-state flux,  $t$  is time and  $K$  is a constant whose dimension depends on the values of  $n$ .  $n$  in both two models is the general index which depending on the fouling mechanism assumes different values.

When  $n$  corresponds to 2, the complete blocking model is assumed, that is, each particle when arriving at the membrane surface blocks some membrane pores such that no superposition happens, and the blocked surface area is proportional to the permeate volume. In this case, the size of the solute particles is similar to the pore size of the membrane, forming a monomolecular layer on the membrane surface (Equation 4).

$$\ln(J) = \ln J_0 - K_b t \quad (4)$$

In standard pore blocking, the  $n$  value is equal to 1.5, and the solute particles with a smaller size than the pores of the membranes can pass through the membrane pores, reducing the pore size effectiveness (Equation 5).

$$\frac{1}{J^{1/2}} = \frac{1}{J_0^{1/2}} + K_s t \quad (5)$$

when  $n$  is 1, the fouling mechanism represents the incomplete or intermediate blocking model in which the solute particles cannot penetrate completely inside the porous structure, and they can settle on other particles deposited before, forming multilayers (Equation 6).

$$\frac{1}{J} = \frac{1}{J_0} + K_j A t \quad (6)$$

Finally, when the value of  $n$  is 0, the pore blocking is neglected, and it is related to the formation of a cake layer by the accumulation of solute particles onto the membrane surface with a thickness proportional to the permeate volume (Garcia-Ivars et al., 2017) (Equation 7).

$$\frac{1}{J^2} = \frac{1}{J_0^2} + K_c t \quad (7)$$

To evaluate the combined effect of the different pore blocking and the filtration layer was used a model suggested by Ho and Zydney (2000), according to Equation 8.

$$Q = Q_0 \left[ \exp\left(-\frac{\alpha \Delta PC}{\mu R_m} t\right) + \frac{R_m}{R_m + R_p} X \left(1 - \exp\left(-\frac{\alpha \Delta PC}{\mu R_m} t\right)\right) \right] \quad (8)$$

where  $Q_0$  is the initial flow rate ( $\text{m}^3 \cdot \text{s}^{-1}$ ),  $\alpha$  is the pore blockage parameter ( $\text{m}^2 \cdot \text{kg}^{-1}$ ),  $\Delta P$  is the transmembrane pressure (Pa),  $C$  is the bulk concentration s,  $\mu$  is the permeate viscosity (Pa.s),  $R_m$  is the membrane resistance ( $\text{m}^{-1}$ ), and  $t$  is the filtration time (s).

Different resistances can appear throughout the process when a complex solution is used as the feed solution (Leu et al., 2017). The sum of these resistances is represented by a total resistance  $R_t$  ( $\text{m}^{-1}$ ) (Equation 9).

$$R_t = R_m + R_r + R_{ir} \quad (9)$$

The  $R_t$  was calculated according to Equation 10:

$$R_t = \frac{P}{\mu_w J_f} \quad (10)$$

where  $J_f$  ( $\text{L} \cdot \text{h}^{-1} \cdot \text{m}^{-2}$ ) is the final permeate flow, the permeate viscosity was considered to be similar to that of water  $\mu_w$  ( $\text{mPa} \cdot \text{s}^{-1}$ ) and the experimental pressure  $P$  (Pa) was controlled. The membrane resistance  $R_m$  ( $\text{m}^{-1}$ ) was obtained from Equation 11 by permeating pure water through the nanofiltration membrane. The viscosity of water  $\mu_w$  ( $\text{mPa} \cdot \text{s}^{-1}$ ) and the permeate flow  $J_w$  ( $\text{L} \cdot \text{h}^{-1} \cdot \text{m}^{-2}$ ) were considered before the process with the skim milk.

$$R_m = \frac{P}{\mu_w J_w} \quad (11)$$

The irreversible fouling resistance  $R_{ir}$  ( $\text{m}^{-1}$ ) was obtained after filtration of the skimmed goat milk by Equation 12. The skimmed goat milk was removed, and pure water was fed into the system to obtain the water permeate flow  $J_{wf}$  ( $\text{L} \cdot \text{h}^{-1} \cdot \text{m}^{-2}$ ).

$$R_{ir} = \frac{P}{\mu_w J_{wf}} \quad (12)$$

The reversible resistance  $R_r$  ( $\text{m}^{-1}$ ) was obtained by difference, as shown in Equation 13.

$$R_r = R_t - R_m - R_{ir} \quad (13)$$

For adjusting all the equations, a computer routine for Matlab (R2013a, MathWorks Inc, MA, USA) was developed, using the `nlinfit` function.

### 2.3 Physicochemical analysis

All the physicochemical analyses were realized in the initial skimmed goat milk, retentate e permeate from the nanofiltration process, and were carried out in triplicate. The total solids content ( $\text{g} \cdot 100 \text{g}^{-1}$ ) was determined through the drying of the samples until reaching a constant weight at  $105^\circ \text{C}$  (Instituto Adolfo Lutz,

2008) and the total protein, by the Kjeldahl method ( $\text{N} \times 6.38$ ) (Association of Official Analytical Chemists, 2012). The lactose content ( $\text{g} \cdot 100 \text{g}^{-1}$ ) was obtained using a spectrophotometer FT-NIR model MPA (Multi-Purpose Analyzer) (Bruker Optik, Ettlingen, Germany) operating with a spectral acquisition program OPUS version 7.0 (Bruker Optik, Ettlingen, Germany). The measurements were made by near-infrared Fourier transform (FTNIR) spectra of diffuse reflectance. Each vial containing the samples was positioned in the diffuse reflectance accessory and the NIR spectra were collected in the spectral range of  $9.000$  to  $4.000 \text{ cm}^{-1}$  at a nominal resolution of  $16 \text{ cm}^{-1}$  in transmission mode. Each spectrum was the average of 500 scans.

The ash content ( $\text{g} \cdot 100 \text{g}^{-1}$ ) was analyzed through a gravimetric method (Instituto Adolfo Lutz, 2008). The mineral content of Ca, Mg, Zn, Mn, Cu, and Co ( $\text{mg} \cdot 100 \text{g}^{-1}$ ) were determined by flame atomic absorption spectrometry (F-AAS) according to Navarro-Alarcón et al. (2011), with modifications. The spectrometer used was the AAnalyst 200 model (PerkinElmer, Inc., Waltham, MA, EUA) equipped with the background corrector with the deuterium arc illumination and the Echelle resolution system. Acetylene (purity 99.7%) was used as fuel gas to heat the atomization system and as compressed gas, compressed air was used. Before de measurement, all samples were calcined at  $520^\circ \text{C}$  and the ash treated using hydrochloric acid  $8 \text{ mol L}^{-1}$ . The analytical and instrumental parameters were adjusted to obtain the best sensitivity for each element. For this, the samples were diluted with Milli-Q water for interpolation in the linear range of each element. The wavelengths used to determine the elements were  $422.67 \text{ nm}$  for Ca,  $285.21 \text{ nm}$  for Mg,  $213.86 \text{ nm}$  for Zn,  $279.50 \text{ nm}$  for Mn,  $324.80 \text{ nm}$  for Cu, and  $240.73 \text{ nm}$  for Co using cathode lamps (PerkinElmer, Inc., Waltham, MA, USA).

### 2.4 Rheological properties

The measurements of rheological properties of skimmed goat milk, retentate and permeate were carried out using a Thermo Haake DC 10 rotational viscosimeter (model VT 550, Thermo Haake, Karlsruhe, Germany), with concentric cylinders (NV ST 807-0713 CE and NV 807-0702) and collected using the software program Pro Rheowin® (version 2.93, Haake). The control of temperature ( $5^\circ \text{C}$ ) was realized through water circulation in a temperature-controlled bath (Phoenix P1, Thermo Haake, Karlsruhe, German) and coupled to the equipment. An aliquot volume of  $10 \text{ mL}$  of samples was loaded into the cup of viscometer and the data were obtained. The flow curves were generated by a linearly increased shear rate of  $0 \text{ s}^{-1}$  to  $2000 \text{ s}^{-1}$  (upward curve) and  $2000 \text{ s}^{-1}$  to  $0 \text{ s}^{-1}$  (downward curve) for 3 minutes. To accurately evaluate the most adapted flow behavior, the models most frequently employed in food characterization (Vélez-Ruiz et al., 1997) were used to describe the shear rate-shear stress data expressed by Equations 14 and 15.

$$\text{Power-law: } \sigma = K(\dot{\gamma})^n \quad (14)$$

$$\text{Herschel-Bulkley: } \sigma = \sigma_0 + K\dot{\gamma}^n \quad (15)$$

where  $\sigma$  is shear stress (Pa),  $\dot{\gamma}$  is the shear rate ( $\text{s}^{-1}$ ),  $K$  is consistency index ( $\text{Pa} \cdot \text{s}^{-1}$ ),  $n$  is flow behavior index, and  $\sigma_0$  is yield stress (Pa).

## 2.5 Statistical analysis

The results were expressed as means  $\pm$  standard deviations and were evaluated using the software STATISTICA version 13.3 (TIBCO Software Inc., Palo Alto, CA). Both one-way analysis of variance (ANOVA) and Tukey's studentized range ( $P < 0.05$ ) was carried out to test for any significant differences between the results.  $R^2$  values were calculated for the fit of the model's data.

## 3 Results and discussion

### 3.1 Nanofiltration process

Figure 1a shows the permeate flux as a function of operating time, for the nanofiltration process using skimmed goat as feed solutions. Two stages can be distinguished, evidencing the membrane fouling during nanofiltration processes of the skimmed goat milk. The initial decline of permeate flux values visualizes on the first minutes of the process is related to the solute particles accumulated and adsorbed onto the surface and inside the pore walls, known as concentration by polarization. According to Ng et al. (2017), the concentration polarization occurs, in the case of skimmed milk, due to the presence of proteins and minerals. Milk proteins foul the membrane by adsorbing to and depositing onto the membrane surface and creating a flux resistance in the form of a gelatinous cake layer (Rice et al., 2009). This protein adsorption is influenced by electrostatic effects between the charged protein and charged membrane, and by the hydrophobicity of the membrane. Rice et al. (2009) stated that calcium can contribute to this protein cake by forming protein-protein and protein-membrane bridges. Meanwhile, soluble ions can precipitate once their solubility is exceeded, potentially forming a scale within the pores or on the surface of the membrane. Calcium phosphate salts are of particular concern in the dairy industry due to their supersaturation in the aqueous phase of milk. This phenomenon increases the osmotic pressure of the solution, resulting in a significant decrease of the flow so that the system must be stopped, as observed in the second stage of permeate flux in Figure 1a, where a gradual flux

decline at more extended periods, up to VRF equal to 2. In this VRF the equilibrium between the attachment and detachment of skimmed goat milk particles on the membrane was reached, achieving an almost constant value of the permeate flux. The mechanisms involved in this process can promote higher concentrations of some constituents next to the membrane surface and, consequently, adhere to the surface and creating a resistance to fluid flow.

During a fouling experiment, the resistance to the fluid flow increases due to various mechanisms, such as pore plugging, cake layer formation, concentration polarization, and osmotic pressure. Skimmed milk filtration is particularly susceptible to poor operational efficiency due to flux decline resulting from concentration polarization and fouling. The resistance by concentration polarization is the accumulation of retained particles at the membrane surface and is responsible for the most of reversible resistances. While resistance by fouling occurs due to adsorption or deposition of colloidal particles on the membrane surface and in the membrane pores and is responsible for the irreversible resistance (Ng et al., 2017). In the present study, the reversible resistance contributed to 98.30% of total resistance, while the membrane and the irreversible resistance contributed to 1.2 and 0.4%, respectively. Rezzadori et al. (2014) cited this processes operating at pressures above 3 bar are more susceptible to the deposition of solutes on the membrane surface, this deposition being related to the concentration by polarization layer, corroborating with the results described in this study. The reversible resistance is a direct result of flux and is usually reversible in the sense that it will quickly diffuse if flux across the membrane is halted. However, if the reversible resistance is high, as observed in this study, a gel layer may be formed by particle-particle interactions and such layer dissipates slowly, if at all, when the flux is interrupted (Ng et al., 2018). From an operational perspective, the reversible resistance is unavoidable, but it can be minimized by improving particle convection away from the membrane (Brans et al., 2004). On the other hand, irreversible resistance fouling is irreversible (upon cessation of flux), and its

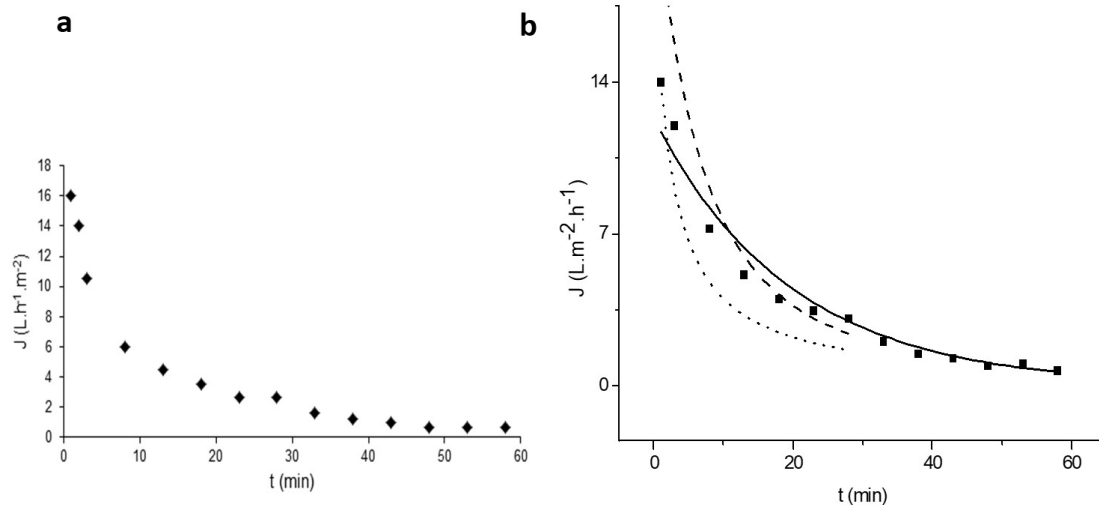


**Figure 1.** Behavior of (a) permeate flux curve (◆) and (b) permeate flux experimental (■) by the complete pore blocking model (—), standard pore blocking (---), and intermediate pore blocking (- - -) from nanofiltration of skimmed goat milk processes up to volume reduction factor (VRF) equal to 2 at 700kPa and  $25 \pm 1$  °C.

removal requires backwashing or often even chemical cleaning. This interrupts operation, lowers productivity, consumes large amounts of water and chemicals, and decreases membrane life (Brans et al., 2004). Rabiller-Baudry et al. (2002) identified in the ultrafiltration of skimmed milk that the adsorption of all milk components (lactose, salts, proteins), even under static conditions. However, after rinsing, lactose and salts were removed, but proteins remained adhered to the membrane. Hence, lactose and salts play a role in reversible resistance, whereas proteins take part in both resistances (reversible and irreversible).

The membrane fouling mechanism during the nanofiltration process of the skimmed goat milk up to VRF of 2 was estimated by Hermia's model, and the fitting of the models was evaluated in the light of the  $R^2$ . The results of the sample calculations for the studied model with the experimental results are shown in Table 1 and Figure 1b. According to Razi et al. (2012), the resistance coefficient (K) is dependent on the resistance and concentration of the filter cake layer and blocked surface, mostly being influenced by the system pressure. The highest resistance coefficient was obtained for the complete pore blocking models, while the best fit ( $R^2$ ) was obtained for the standard and complete pore blocking models, with  $R^2 \geq 0.97$ . Vincent Vela et al. (2009) stated that adsorptive fouling of membranes by particles smaller than the membrane pore sizes is incorporated in the standard blocking model. Therefore, particles may deposit inside the membrane pore walls, leading to the reduction of the cross-sectional area of membrane pores and a consequent increase in membrane resistance. This fouling phenomenon always operates in non-steady-state conditions, and it is independent of the crossflow rate. In the nanofiltration process of skimmed goat milk, this behavior could be occurring by the deposit of whey protein and some minerals that have a lower size than the membrane pore. According to Corbatón-Báguena et al. (2015), it is important to note that one of the hypotheses of Hermia's complete blocking model is that the pore entrance is completely blocked or sealed when one solutes molecule arrives at the membrane surface. Therefore, complete blocking considers membrane fouling mechanisms that are external and occur on the membrane surface. These external membrane fouling mechanisms are related to the difference between the solute molecule size and the membrane pore size. Consequently, particles/solutes do not permeate through the membrane, such as casein, lactose, phosphate minerals, and minerals bound to casein micelles. By the obtained results, it was established that in the early stage the rapid permeate flux decline of the nanofiltration process was characterized initially by a standard blocking model and subsequently, by a complete blocking model.

**Table 1.** Phenomenological constant (K) and  $R^2$  values from the fouling mechanism of the skimmed goat milk nanofiltration up to volume reduction factor (VRF) equal to 2.

Fouling mechanism	K	R2
Complete blocking (n = 2) ( $s^{-1}$ )	0.051	0.98
Standard blocking (n = 1.5) ( $m^{-0.5} s^{-0.5}$ )	0.016	0.97
Incomplete blocking (n = 1) ( $m^{-1}$ )	0.015	0.86

K = resistance coefficient;  $R^2$  = determination coefficient.

Ng et al. (2017) affirm that a single fouling model did not provide a good description of the entire filtration process. A combined fouling model which considers both pore blocking and cake formation may be more appropriate, such as the transient area-averaged protein filtration model developed by Ho & Zydney (2000).

The data and model predictions are shown in Figure 2. The model calculations were in good agreement with the experimental data over the entire nanofiltration period, showing an  $R^2 > 0.97$ . Corbatón-Báguena et al. (2015) stated that in this model are considered the two stages in the decrease in permeate flux with time: a rapid flux decline due to pore-blocking phenomena and, after that, a slow decrease until the steady-state is achieved due to the formation of a cake layer. According to Torkamanzadeh et al. (2016), the hypothesis assumed in this model is that by deposition of the first protein aggregates on the membrane surface, the blocked pores will still be partially permeable to the fluid flow. The model also accounts for the nonuniform character of foulant particle deposition over the surface of the membrane. Li et al. (2017) suggest the fouling mechanism in the filtration of concentrated milk is not purely cake formation or protein deposition, but a combination of both, influenced by operating conditions and evolution of the feed composition. Besides the protein deposition, mineral fouling by dairy streams is attributed to the precipitation of calcium phosphate as it is sparingly soluble. Skim milk is supersaturated concerning calcium phosphate, but precipitation of calcium phosphate does not occur naturally. This is mainly due to associations with casein micelles, which provide a sufficient buffering capacity for calcium phosphate (Ng et al., 2018). In addition, NF membrane pores are smaller than mineral ions, thus fouling by calcium phosphate precipitation in the bulk fluid could occur during skimmed milk nanofiltration.

### 3.2 Physicochemical properties

The total solids, protein, and lactose content of skimmed goat milk, retentate and permeate are shown in Table 2. It was possible to note that the nanofiltration process was successfully

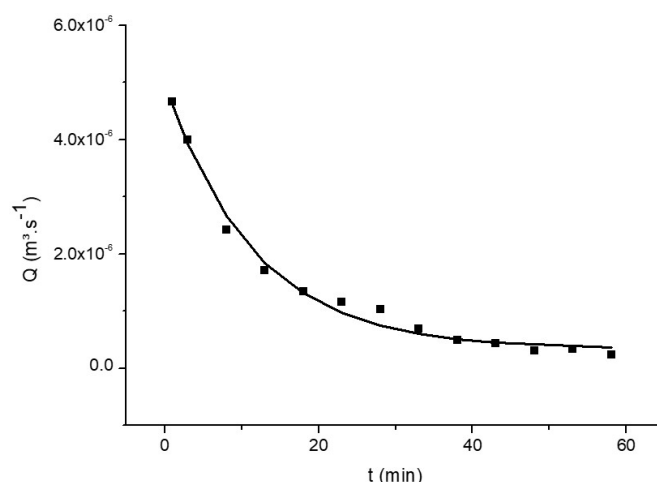


**Figure 2.** Permeate flux experimental (■) by the combined model (—) from nanofiltration of skimmed goat milk processes up to volume reduction factor (VRF) equal to 2 at 700kPa and  $25 \pm 1$  °C.

**Table 2.** Total solids, protein, lactose, ash content (g 100 g<sup>-1</sup>) and mineral fractions (mg 100 g<sup>-1</sup>) of skimmed goat milk, retentate and permeate from nanofiltration up to volume reduction factor (VRF) equal to 2.

Analyses	Skimmed goat milk	Retentate	Permeate
Total solids (g 100 g <sup>-1</sup> )	8.46 ± 0.01 <sup>b</sup>	13.46 ± 0.08 <sup>a</sup>	1.00 ± 0.01 <sup>c</sup>
Total protein (g 100 g <sup>-1</sup> )	2.91 ± 0.05 <sup>b</sup>	4.41 ± 0.02 <sup>a</sup>	0.24 ± 0.01 <sup>c</sup>
Lactose (g 100 g <sup>-1</sup> )	3.93 ± 0.05 <sup>b</sup>	8.10 ± 0.32 <sup>a</sup>	ND
Ash (g 100g <sup>-1</sup> )	0.96 ± 0.03 <sup>b</sup>	1.22 ± 0.01 <sup>a</sup>	0.45 ± 0.01 <sup>c</sup>
Ca (mg 100g <sup>-1</sup> )	9874.80 ± 3.38 <sup>b</sup>	19266.85 ± 34.77 <sup>a</sup>	848.45 ± 0.36 <sup>c</sup>
Mg (mg 100g <sup>-1</sup> )	825.16 ± 1.21 <sup>b</sup>	1801.00 ± 0.15 <sup>a</sup>	99.94 ± 0.01 <sup>c</sup>
Zn (mg 100g <sup>-1</sup> )	69.71 ± 0.03 <sup>a</sup>	41.91 ± 0.01 <sup>c</sup>	42.12 ± 0.03 <sup>b</sup>
Cu (mg 100g <sup>-1</sup> )	2.99 ± 0.01 <sup>c</sup>	3.80 ± 0.01 <sup>b</sup>	10.10 ± 0.01 <sup>a</sup>
Mn (mg 100g <sup>-1</sup> )	0.21 ± 0.01 <sup>c</sup>	2.05 ± 0.01 <sup>a</sup>	0.62 ± 0.01 <sup>b</sup>
Co (mg 100g <sup>-1</sup> )	0.869 ± 0.01 <sup>a</sup>	0.665 ± 0.01 <sup>b</sup>	0.276 ± 0.01 <sup>c</sup>

<sup>a-c</sup>Within a row, means ± standard deviations with different superscript lowercase letters denote significant differences ( $P < 0.05$ ) between the skimmed goat milk and retentates and permeates from nanofiltration (NF). VRF: volume reduction factor.

**Table 3.** Rheological parameters obtained using Power Law ( $\sigma = K(\dot{\gamma})^n$ ) and Herschell-Buckley model ( $\sigma = \sigma_0 + k\dot{\gamma}^n$ ) of skimmed goat milk and retentate from nanofiltration up to volume reduction factor (VRF) equal to 2 at 5.0 ± 0.1 °C.

Samples	Power Law model			Herschell-Buckley model			
	K (Pa.s <sup>n</sup> )	n	R <sup>2</sup>	$\sigma_0$	K (Pa.s <sup>n</sup> )	n	R <sup>2</sup>
Skimmed goat milk	0.003 ± 0.003 <sup>ab</sup>	0.920 ± 0.029 <sup>b</sup>	0.955	0.012 ± 0.002 <sup>c</sup>	0.003 ± 0.001 <sup>ab</sup>	0.927 ± 0.031 <sup>b</sup>	0.955
Retentate	0.005 ± 0.001 <sup>a</sup>	0.922 ± 0.002 <sup>b</sup>	0.968	0.047 ± 0.001 <sup>b</sup>	0.004 ± 0.001 <sup>a</sup>	0.946 ± 0.015 <sup>b</sup>	0.965
Permeate	0.002 ± 0.001 <sup>b</sup>	0.976 ± 0.003 <sup>a</sup>	0.850	0.092 ± 0.001 <sup>a</sup>	0.001 ± 0.001 <sup>b</sup>	1.006 ± 0.012 <sup>a</sup>	0.851

<sup>a-c</sup>Within a column, means ± standard deviations with different superscript lowercase letters denote significant differences ( $P < 0.05$ ) between the skimmed goat milk and retentates and permeates from nanofiltration (NF). VRF: volume reduction factor; K, Consistency index; n, flow behavior index; R<sup>2</sup>, determination coefficient;  $\sigma_0$ , yield stress.

employed for concentrating on total solids, protein, and lactose content ( $P < 0.05$ ) from skimmed goat milk indicated that the skimmed goat milk molecular size in the great majority is larger than nanofiltration membrane pore size. The total solids content determined to retentate in this study was higher than that found by Moreno-Montoro et al. (2015), in the ultrafiltration of skimmed goat milk. However, in the present study, some protein molecules do pass through the membrane due to dehydration. The concentration of protein is important, which is advantageous for dairy production given that they are the most important proteins for curd formation in the fermentation process. Casein and whey protein are valuable food ingredients because of their nutritive value and physicochemical and functional properties. Due to their water-binding, emulsifying, whipping, foaming, and texturizing properties, they are used in a range of commercial applications, including protein fortification of dairy foods, and ingredients for beverages, bakery, and meat (Sauer et al., 2012). The nanofiltration process was also efficient in the concentration of lactose content, once cannot be quantified in permeate, been predominantly in the retentate.

The nanofiltration process contributed to the increase ( $P < 0.05$ ) of the ash and mineral fractions of retentate (Table 2). Concerning mineral fraction, Ca, Mg, and Mn showed the highest ( $P < 0.05$ ) values in the retentate. However, Zn content was presented in the retentate and permeate with similar values. Cu showed higher ( $P < 0.05$ ) values in the permeate, while the Co was lower ( $P < 0.05$ ) in the retentate and permeate about skimmed goat milk. These behaviors were related to the size of

the molecules and the deposit of part of these minerals in the pore walls.

Concerning the rheological properties, Figure 3 shows the differences between the apparent viscosity behaviors of skimmed goat milk, retentate and permeate. The skimmed goat milk and retentate showed a slight decrease in apparent viscosity with increasing the shear rate, indicated that these fluids had shear thinning characteristics (non-Newtonian behavior). Showing a different behavior, the permeate exhibited a Newtonian behavior. Vélez-Ruiz & Barbosa-Cánovas (1998) related the Newtonian behavior of permeate to the low solids concentrations of these samples (Table 2). It was also possible to observe that the apparent viscosity was higher ( $P < 0.05$ ) for the retentate. In the concentration of skimmed milk, the increase of viscosity occurs because the removal of water causes an increase in volume fraction of dispersed particles and increases the micelle-micelle interactions as the distance between the micelles becomes smaller.

According to Balde & Aider (2016) and Vélez-Ruiz & Barbosa-Cánovas, (1998) the milk concentrates behaved as non-Newtonian fluids, with flow curves well fitted by the Power law and/or Herschel-Bulkley models as observed in the present study for the skimmed goat milk and retentate, with showed a coefficient of determination (R<sup>2</sup>) higher than 0.95 (Table 3). The rheological behavior of a fluid can also be described by the consistency coefficient (K), and the flow behavior index (n). When the e n value is close to 1, the sample showed Newtonian behavior and n is less than 1, the sample shear thins with increasing shear rate, whereas if n is higher than 1, the sample shear thickens.

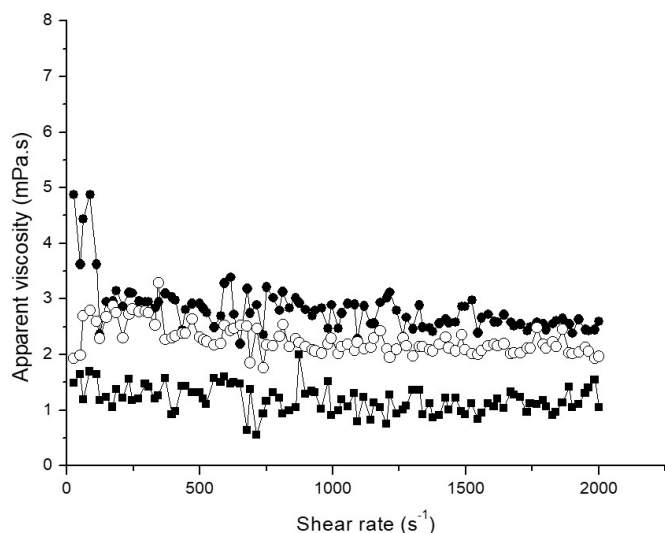


**Figure 3.** Apparent viscosity versus shear rate of (○) skimmed goat milk (●) retentate and (■) permeate from nanofiltration up to volume reduction factor (VRF) equal to 2.

Both models used showed the higher flow behavior index ( $n$ ), confirming the Newtonian behavior presented in Figure 3. The yield stress ( $\sigma_0$ ) were of the samples was close to 0. According to Balde & Aider (2016) and Canella et al. (2019), when the total solid content of the skimmed milk is lower than 30 g 100 g<sup>-1</sup> the yield stress presented lower values.

The above experimental results and analysis suggest that nanofiltration is an interesting technology for skimmed milk concentration. Moreover, it is important to determine the flow decline behavior since the resistances visualized throughout the process had a direct influence on the retention of the constituents and the process performance.

#### 4 Conclusions

During the nanofiltration process of the skimmed goat milk was observed at the low time a rapid decrease of the permeate flux. At a long time of the nanofiltration process, it was verified a continuous flux, which was characterized by an additional resistance to the permeate flux caused by concentration polarization. For the VRF value equal to 2, the standard and complete blocking were the best fitting modes. The conclusions obtained from a combined model based on the crossflow of the permeate flux decline along the whole filtration curve were that the reversible resistance was the main responsible for the flux decline and the rapid permeate flux decline in the early stage of the nanofiltration process was characterized by standard and complete blocking. The combined model calculations were in good agreement with the experimental data over the entire nanofiltration period. It was determined that the nanofiltration process be successfully employed to concentrate total solids, protein, lactose, ash, and mineral fractions. The Power Law and Herschel-Buckley models were fitting to describe the flow behavior for retentate, which presented the higher apparent viscosity. Finally, these findings not only clarify the fouling mechanism involved during the nanofiltration process of the skimmed goat milk but also provide

valuable knowledge about the concentration of its components that can be used by the dairy industry. These high values prove the potential of this technology for use as a pre-concentration step, aiming to obtain a product with the sensory and nutritional qualities preserved with lower production costs.

#### Acknowledgements

The authors are grateful to the Coordination of Improvement of Higher Education Personnel by scholarship (CAPES, Finance code-001) and the National Council of Technological and Scientific Development by the financial support (CNPq, 405965/2016-8). Elane Schwinden Prudencio and Erick Almeida Esmerino have a research grant from CNPq.

#### References

- Association of Official Analytical Chemists – AOAC. (2012). *Official methods of analysis* (19th ed.). Gaithersburg: AOAC International.
- Balde, A., & Aider, M. (2016). Impact of cryoconcentration on casein micelle size distribution, micelles inter-distance, and flow behavior of skim milk during refrigerated storage. *Innovative Food Science & Emerging Technologies*, 34, 68-76. <http://dx.doi.org/10.1016/j.ifset.2015.12.032>.
- Balyan, U. B., & Sarkar, B. (2018). Analysis of flux decline using sequential fouling mechanisms during concentration of *Syzygiumcumini* (L.) leaf extract. *Chemical Engineering Research & Design*, 130, 167-183. <http://dx.doi.org/10.1016/j.cherd.2017.12.015>.
- Brans, G., Schroën, C. G. P. H., van der Sman, R. G. M., & Boom, R. M. (2004). Membrane fractionation of milk: state of the art and challenges. *Journal of Membrane Science*, 243(1-2), 263-272. <http://dx.doi.org/10.1016/j.memsci.2004.06.029>.
- Canella, M. H. M., Muñoz, I. B., Barros, E. L. S., Silva, C. C., Ploêncio, L. A. S., Daguier, H., & Prudencio, E. S. (2019). Block freeze concentration as a technique aiming the goat milk concentration: fate of physical, chemical, and rheological properties. *International Journal of Engineering Sciences & Research Technology*, 8, 87-104.
- Carvalho, S. G., Oliveira, J. S., Saraiva, C. A. S., Santos, E. M., Vieira, D. S., Cruz, A. F., Torres, P. C. Jr., Albuquerque, Í. R. R., Araújo, A. O., & Ribeiro, N. L. (2023). Sensory analysis of goat cheese feed with sorghum silage levels in forage cactus based diets. *Food Science and Technology*, 43, e90022. <http://dx.doi.org/10.1590/fst.90022>.
- Chen, D., Li, X., Zhao, X., Qin, Y., Wang, J., & Wang, C. (2019). Comparative proteomics of goat milk during heated processing. *Food Chemistry*, 275, 504-514. <http://dx.doi.org/10.1016/j.foodchem.2018.09.129>. PMID:30724227.
- Corbatón-Báguena, M. J., Álvarez-Blanco, S., & Vincent-Vela, M. C. (2015). Fouling mechanisms of ultrafiltration membranes fouled with whey model solutions. *Desalination*, 360, 87-96. <http://dx.doi.org/10.1016/j.desal.2015.01.019>.
- Ferrer, M., Alexander, M., & Corredig, M. (2014). Changes in the physico-chemical properties of casein micelles during ultrafiltration combined with diafiltration. *Lebensmittel-Wissenschaft + Technologie*, 59(1), 173-180. <http://dx.doi.org/10.1016/j.lwt.2014.04.037>.
- Field, R. W., Wu, D., Howell, J. A., & Gupta, B. B. (1995). Critical flux concept for microfiltration fouling. *Journal of Membrane Science*, 100(3), 259-272. [http://dx.doi.org/10.1016/0376-7388\(94\)00265-Z](http://dx.doi.org/10.1016/0376-7388(94)00265-Z).
- Garcia-Ivars, J., Martella, L., Massella, M., Carbonell-Alcaina, C., Alcaina-Miranda, M. I., & Iborra-Clar, M. I. (2017). Nanofiltration as tertiary treatment method for removing trace pharmaceutically

- active compounds in wastewater from wastewater treatment plants. *Water Research*, 125, 360-373. <http://dx.doi.org/10.1016/j.watres.2017.08.070>. PMID:28881212.
- Haenlein, G. F. W. (2004). Goat milk in human nutrition. *Small Ruminant Research*, 51(2), 155-163. <http://dx.doi.org/10.1016/j.smallrumres.2003.08.010>.
- Hariadi, H., Rukmana, J., Endah Rohima, I., Marthia, N., Nurminabari, I. S., Nurhawa, S., Nadhirah, T. D., & Fadhila, R. N. (2023a). Study of drying temperature variation and concentration green spinach (*Amaranthus Hybridus* l) on characteristics of spinach milk powder. *Food Science and Technology*, 43, e110722. <http://dx.doi.org/10.1590/fst.110722>.
- Hariadi, H., Sagita, D., Rahmawati, L., Triyono, A., Hidayat, Mayasti, N. K. I., Kurniawan, K., Purwandoko, P. B., Anggara, C. E. W., & Andriansyah, R. C. (2023b). Study of addition sweet potato extract on sensory test and antioxidant activity in yoghurt. *Food Science and Technology*, 43, e88422. <http://dx.doi.org/10.1590/fst.88422>.
- Hermia, J. (1982). Constant pressure blocking filtration laws: applications to power-law non-Newtonian fluids. *Icheme*, 60, 183-187.
- Ho, C. C., & Zydney, A. L. (2000). A combined pore blockage and cake filtration model for protein fouling during microfiltration. *Journal of Colloid and Interface Science*, 232(2), 389-399. <http://dx.doi.org/10.1006/jcis.2000.7231>. PMID:11097775.
- Hou, L., Wang, Z., & Song, P. (2017). A precise combined complete blocking and cake filtration model for describing the flux variation in membrane filtration process with BSA solution. *Journal of Membrane Science*, 542, 186-194. <http://dx.doi.org/10.1016/j.memsci.2017.08.013>.
- Instituto Adolfo Lutz – IAL. (2008). *Normas analíticas do Instituto Adolfo Lutz: métodos físico-químicos para análise de alimentos* (4<sup>a</sup> ed.). São Paulo: IAL.
- Leu, M., Marciniak, A., Chamberland, J., Pouliot, Y., Bazinet, L., & Doyen, A. (2017). Effect of skim milk treated with high hydrostatic pressure on permeate flux and fouling during ultrafiltration. *Journal of Dairy Science*, 100(9), 7071-7082. <http://dx.doi.org/10.3168/jds.2017-12774>. PMID:28647330.
- Li, H., Hsu, Y. C., Zhang, Z., Dharsana, N., Ye, Y., & Chen, V. (2017). The influence of milk components on the performance of ultrafiltration/diafiltration of concentrated skim milk. *Separation Science and Technology*, 52(2), 381-390. <http://dx.doi.org/10.1080/01496395.2016.1217243>.
- Moreno-Montoro, M., Olalla, M., Giménez-Martínez, R., Bergillos-Meca, T., Ruiz-López, M. D., Cabrera-Vique, C., Artacho, R., & Navarro-Alarcón, M. (2015). Ultrafiltration of skim goat milk increases its nutritional value by concentrating nonfat solids such as proteins, Ca, P, Mg, and Zn. *Journal of Dairy Science*, 98(11), 7628-7634. <http://dx.doi.org/10.3168/jds.2015-9939>. PMID:26342988.
- Navarro-Alarcón, M., Cabrera-Vique, C., Ruiz-López, M. D., Olalla, M., Artacho, R., Giménez, R., Quintana, V., & Bergillos, T. (2011). Levels of Se, Zn, Mg and Ca in commercial goat and cow milk fermented products: relationship with their chemical composition and probiotic starter culture. *Food Chemistry*, 129(3), 1126-1131. <http://dx.doi.org/10.1016/j.foodchem.2011.05.090>. PMID:25212347.
- Ng, K. S. Y., Dunstan, D. E., & Martin, G. J. O. (2018). Influence of processing temperature on flux decline during skim milk ultrafiltration. *Separation and Purification Technology*, 195, 322-331. <http://dx.doi.org/10.1016/j.seppur.2017.12.029>.
- Ng, K. S. Y., Haribabu, M., Harvie, D. J. E., Dunstan, D. E., & Martin, G. J. O. (2017). Mechanisms of flux decline in skim milk ultrafiltration: A review. *Journal of Membrane Science*, 523, 144-162. <http://dx.doi.org/10.1016/j.memsci.2016.09.036>.
- Rabiller-Baudry, M., Le Maux, M., Chaufer, B., & Begoin, L. (2002). Characterization of cleaned and fouled membrane by ATR-FTIR and EDX analysis coupled with SEM: application to UF of skimmed milk with a PES membrane. *Desalination*, 146(1-3), 123-128. [http://dx.doi.org/10.1016/S0011-9164\(02\)00503-9](http://dx.doi.org/10.1016/S0011-9164(02)00503-9).
- Razi, B., Aroujalian, A., & Fathizadeh, M. (2012). Modeling of fouling layer deposition in cross-flow microfiltration during tomato juice clarification. *Food and Bioproducts Processing*, 90(4), 41-48. <http://dx.doi.org/10.1016/j.fbp.2012.05.004>.
- Rezzadori, K., Serpa, L., Penha, F. M., Petrus, R. R., & Petrus, J. C. C. (2014). Crossflow microfiltration of sugarcane juice: Effects of processing conditions and juice quality. *Food Science and Technology*, 34(1), 210-217. <http://dx.doi.org/10.1590/S0101-20612014000100030>.
- Ribeiro, J. E. S., Sant'Ana, A. M. S., Silva, F. L. H., & Beltrão, E. M. Fo. (2023). Use of water-soluble soy extract and inulin as ingredients to produce a fermented dairy beverage made from caprine milk. *Food Science and Technology*, 43, e102122. <http://dx.doi.org/10.1590/fst.102122>.
- Rice, G., Barber, A., O'Connor, A., Stevens, G., & Kentish, S. (2009). Fouling of NF membranes by dairy ultrafiltration permeates. *Journal of Membrane Science*, 330(1-2), 117-126. <http://dx.doi.org/10.1016/j.memsci.2008.12.048>.
- Santos, W. F., Cruz, R. B., Costa, R. G., Ribeiro, N. L., Beltrão, E. M. Fo., Sousa, S., Justino, E. S., & Santos, D. G. (2022). Production and quality of cheese and milk of goats fed with guava agroindustrial waste (*Psidium guajava* L.). *Food Science and Technology*, 42, e00521. <http://dx.doi.org/10.1590/fst.00521>.
- Sauer, A., Doehner, I., & Moraru, C. I. (2012). Steady shear rheological properties of micellar casein concentrates obtained by membrane filtration as a function of shear rate, concentration, and temperature. *Journal of Dairy Science*, 95(10), 5569-5579. <http://dx.doi.org/10.3168/jds.2012-5501>. PMID:22901476.
- Silva, A. C. V., Ramos, G. L. P. A., Ferreira, P. S., & Silva, M. C. (2023). Technological prospection of aquafaba: a study of patent applications and trends in the food Market. *Food Science and Technology*, 43, e114422. <http://dx.doi.org/10.1590/fst.114422>.
- Sobral, G. C., Oliveira, J. S., Saraiva, C. A. S., Santos, E. M., Vieira, D. S., Cruz, A. F., Torres, P. C. Jr., Albuquerque, Í. R. R., Araújo, A. O., & Ribeiro, N. L. (2023). Sensory analysis of goat cheese feed with sorghum silage levels in forage cactus based diets. *Food Science and Technology*, 43, e90022. <http://dx.doi.org/10.1590/fst.90022>.
- Torkamanzadeh, M., Jahanshahi, M., Peyravi, M., & Rad, A. S. (2016). Comparative experimental study on fouling mechanisms in nanoporous membrane: cheese whey ultrafiltration as a case study. *Water Science and Technology*, 74(12), 2737-2750. <http://dx.doi.org/10.2166/wst.2016.352>. PMID:27997385.
- Vélez-Ruiz, J. F., & Barbosa-Cánovas, G. V. (1998). Rheological properties of concentrated milk as a function of concentration, temperature, and storage time. *Journal of Food Engineering*, 35(2), 177-190. [http://dx.doi.org/10.1016/S0260-8774\(98\)00019-3](http://dx.doi.org/10.1016/S0260-8774(98)00019-3).
- Vélez-Ruiz, J. F., Cánovas, G. V. B., & Peleg, M. (1997). Rheological properties of selected dairy products. *Critical Reviews in Food Science and Nutrition*, 37(4), 311-359. <http://dx.doi.org/10.1080/10408399709527778>. PMID:9227889.
- Vincent Vela, M. C., Álvarez Blanco, S., Lora García, J., & Bergantiños Rodríguez, E. (2009). Analysis of membrane pore blocking models adapted to crossflow ultrafiltration in the ultrafiltration of PEG. *Chemical Engineering Journal*, 149(1-3), 232-241. <http://dx.doi.org/10.1016/j.cej.2008.10.027>.